SUPPLEMENTARY INFORMATION

Table S1. Co-expression of NCAM and FGFR1 in EOC. Cancer biopsies from 77 EOC patients were subjected to immunohistochemical staining for NCAM and FGFR1. 0, no staining; 1, weak staining; 2, moderate staining; 3, intense staining.

Patient number	Tumor histotype	FGFR1	NCAM
1	Adenocarcinoma	3	0
2	Adenocarcinoma	2	0
3	Adenocarcinoma	3	0
4	Adenocarcinoma	3	0
5	Adenocarcinoma	3	0
6	Clear Cell Carcinoma	1	0
7	Endometrioid Adenocarcinoma	3	0
8	Endometrioid Adenocarcinoma	1	0
9	Endometrioid Adenocarcinoma	1	0
10	Endometrioid Adenocarcinoma	3	0
11	Endometrioid Adenocarcinoma	3	3
12	Endometrioid Adenocarcinoma	3	3
13	Endometrioid Adenocarcinoma	2	2
14	Endometrioid Adenocarcinoma	3	0
54	Endometrioid Adenocarcinoma	3	3
55	Endometrioid Adenocarcinoma	1	0
56	Endometrioid Adenocarcinoma	3	0
57	Endometrioid Adenocarcinoma	1	0
19	Mucinous Adenocarcinoma	2	0
20	Mucinous Adenocarcinoma	0	0
21	Mucinous Adenocarcinoma	3	0
22	Mucinous Adenocarcinoma	0	0
23	Mucinous Adenocarcinoma	3	0
24	Mucinous Adenocarcinoma	3	0
25	Mucinous Adenocarcinoma	3	0
26	Serous Adenocarcinoma	3	3
27	Serous Adenocarcinoma	3	0
28	Serous Adenocarcinoma	1	0
29	Serous Adenocarcinoma	3	0
30	Serous Adenocarcinoma	3	0
31	Serous Adenocarcinoma	2	0
32	Serous Adenocarcinoma	3	2
33	Serous Adenocarcinoma	3	0
34	Serous Adenocarcinoma	1	0
35	Serous Adenocarcinoma	1	0
36	Serous Adenocarcinoma	3	2
37	Serous Adenocarcinoma	1	3
38	Serous Adenocarcinoma	3	3
39	Serous Adenocarcinoma	3	0
40	Serous Adenocarcinoma	2	0
41	Serous Adenocarcinoma	3	3

42	Serous Adenocarcinoma	1	0
43	Serous Adenocarcinoma	3	0
44	Serous Adenocarcinoma	1	2
45	Serous Adenocarcinoma	1	0
46	Serous Adenocarcinoma	3	0
47	Serous Adenocarcinoma	1	0
48	Serous Adenocarcinoma	2	0
49	Serous Adenocarcinoma	3	0
50	Serous Adenocarcinoma	3	2
51	Serous Adenocarcinoma	3	0
52	Serous Adenocarcinoma	3	0
53	Serous Adenocarcinoma	1	3
54	Serous Adenocarcinoma	3	3
55	Serous Adenocarcinoma	3	0
56	Serous Adenocarcinoma	1	0
57	Serous Adenocarcinoma	3	0
58	Serous Adenocarcinoma	3	3
59	Serous Adenocarcinoma	3	0
60	Serous Adenocarcinoma	3	0
61	Serous Adenocarcinoma	1	3
62	Serous Adenocarcinoma	3	3
63	Serous Adenocarcinoma	3	0
64	Serous Adenocarcinoma	1	0
65	Serous Adenocarcinoma	3	3
66	Serous Adenocarcinoma	3	0
67	Serous Adenocarcinoma	2	0
68	Serous Adenocarcinoma	3	3
69	Serous Adenocarcinoma	3	0
70	Serous Adenocarcinoma	3	3
71	Serous Adenocarcinoma	3	0
72	Serous Adenocarcinoma	3	2
73	Serous Adenocarcinoma	3	0
74	Serous Adenocarcinoma	3	0
75	Serous Adenocarcinoma	3	0
76	Malignant Mixed Mullerian Tumor	3	3
77	Malignant Mixed Mullerian Tumor	2	3

Supplementary Figure Legends

Fig. S1. Co-expression of NCAM and FGFR1 in EOC tissue. The four panels show representative cores from EOC tissue microarrays stained for NCAM (A, C) or FGFR1 (B, D). Panels A and B provide an example of EOC biopsy in which NCAM and FGFR1 are co-expressed. Panels C and D provide an example in which FGFR1, but not NCAM, is expressed.

Fig. S2. Correlation between the expression of NCAM and of individual FGFR family members in EOC. The co-expression of the NCAM1 gene with the four members of the FGFR family (FGFR1-4) was analysed in a published microarray dataset of 255 EOC patients (GEO accession number GPL7759). Microarray data analysis indicated a significant degree of correlation ($p<0.0001$) between the normalized expression values of NCAM1 and each FGFR gene. Representative graphs indicating the correlations of individual FGFRs with NCAM in EOC microarray datasets are shown in the top panels, while the table shows the results of the statistical analysis (Pearson correlation, 95% CI and relative p-value; analysis performed by Prism software). Analysis of the frequency distribution of the expression values showed that high NCAM expression is always associated with FGFR expression.

Fig. S3. NCAM silencing in MOVCAR cells. MOVCAR cells were transduced with a control short-hairpin RNA (shControl) or with a short-hairpin RNA against mouse NCAM (shNCAM). A set of MOVCAR-shNCAM cells was also reconstituted by transfection with human NCAM (which is not targeted by shNCAM). (A)

Immunofluorescence staining for NCAM (red), showing that shNCAM dramatically reduced the expression of endogenous NCAM. Ectopic expression of human NCAM in shNCAM-transfected cells resulted in reconstitution of NCAM expression and localization at the cell surface. Cells were counterstained with DAPI to visualize nuclei (blue). Scale bar, 10 μm. (B) Immunoblotting for NCAM on lysates from MOVCAR-shControl, MOVCAR-shNCAM and MOVCAR-shNCAM/reconstituted cells (upper panel), confirming the silencing of NCAM expression by shNCAM and its reconstitution upon transfection with human NCAM. Equal loading was verified by immunoblotting for tubulin (lower panel). (C) Cells were incubated in serum-free medium for the indicated time intervals. A set of MOVCAR-shControl cells were also stimulated with 10 ng/ml FGF-2 as indicated. At each time point, cells were fixed and stained with crystal violet. Stained cells were then solubilized with 10% acetic acid, and the absorbance at 595 nm was measured. Values are expressed as arbitrary units referred to the absorbance of MOVCAR-shControl cells at time 0. Error bars represent SEM. *$p<0.05$; **$p<0.005$.

Fig. S4. Ectopic expression of NCAM and ΔFN2 in SKOV3 cells. SKOV3 cells were co-transfected with GFP (green) and with an empty vector, full-length NCAM or NCAM-ΔFN2. (A) Immunofluorescence staining for NCAM (red), showing that both full-length NCAM and ΔFN2 were correctly localized at the cell surface. Cells were counterstained with DAPI to visualize nuclei (blue). Scale bars, 10 μm. (B) Immunoblotting for NCAM on lysates from SKOV3-mock, SKOV3-NCAM and SKOV3-ΔFN2 cells (upper panel), showing that full-length NCAM and ΔFN2 were expressed at similar level. The amount of ectopically expressed GFP was also comparable in all transfectants (lower panel). Equal loading was verified by

immunoblotting for tubulin (middle panel). (C) SKOV3-mock, SKOV3-NCAM and SKOV3-ΔFN2 cells were seeded at a density of 1 x 104 cells per well in 24-well plates, and and subjected to serum starvation. Cells were then stimulated with medium containing 10% FBS for the indicated time lengths, followed by fixation and staining with crystal violet. Stained cells were then solubilized with 10% acetic acid, and the absorbance at 595 nm was measured. Values are expressed as arbitrary units referred to the absorbance of SKOV3-mock cells at time 0. Error bars represent SEM.

Fig. S5. Effect of ectopic expression of NCAM and ΔFN2 on migration and invasion of OVCA433 cells. OVCA433 cells were transfected with an empty vector, full-length NCAM or NCAM-ΔFN2. (A) Immunofluorescence staining for NCAM (red), showing that both full-length NCAM and ΔFN2 were expressed at similar level and correctly localized at the cell surface. Cells were counterstained with DAPI to visualize nuclei (blue). Scale bar, 20 μm. (B) Immunoblotting for NCAM on lysates from OVCA433-mock, OVCA433-NCAM and OVCA433-ΔFN2 cells (upper panel), showing that full-length NCAM and ΔFN2 were expressed at similar level. Equal loading was verified by immunoblotting for actin (lower panel). (C and D) Transfected OVCA433 cells were subjected to migration (C) and Matrigel invasion assays (D). Full-length NCAM, but not ΔFN2, induced OVCA433 cell migration and invasion. Values are expressed as arbitrary units referred to the migration or invasion of OVCA433-mock cells. Error bars represent SEM. *$p<0.005$.

Fig. S6. NCAM interaction with FGFR leads to FGFR activation. (A) Lysates from SKOV3-NCAM and SKOV3-ΔFN2 cells were subjected to immunoprecipitation with anti-FGFR1 or with non-immune rabbit IgG (control IP),

followed by immunoblotting for NCAM (top panels) or FGFR1 (bottom panels). Full-length NCAM, but not of ΔFN2, co-precipitated with FGFR1. Endogenous FGFR1 in SKOV3 cells was detectable only after immunoprecipitation because of the low amount of the receptor. (B) Lysates from SKOV3-mock, SKOV3-NCAM and SKOV3-ΔFN2 cells were immunoblotted for phospho-FGFR (upper panel) and total FGFR1 (lower panel). SKOV3-mock cells were also stimulated with 10 ng/ml FGF-2 for 10 min. prior to lysis, as a positive contro for FGFR phosphorylation. The blots were obtained from the same gel, the white line between the blots indicates the removal of intervening lanes. Ectopic expression of full-length NCAM, but not of ΔFN2, resulted in constitutive FGFR activation. The experiment was repeated three times with similar results. (C) Parental SKOV3 cells were treated with 20 μg/ml Encamin-C for the indicated time lengths, prior to cell lysis and immunoblotting for phospho-FGFR (upper panel) and total FGFR1 (lower panel). Encamin-C induced time-dependent phosphorylation of FGFR. The treatment of SKOV3 cells with a control peptide showed no effect on FGFR phosphorylation (not shown). The experiment was repeated three times with similar results.

Fig. S7. Antibodies 123C3 and Eric-1 interfere with NCAM-mediated activation of FGFR. (A) Recombinant, Fc-tagged NCAM soluble fragments, consisting of the entire ectodomain (NCAM-Fc), the ectodomain lacking the two FN repeats (ΔFN1FN2-Fc), or the isolated FN repeats (FN1FN2-Fc), were resolved in SDS-PAGE and immunoblotted with 123C3 (upper panel) or Eric-1 (middle panel). The blot was also probed with an anti-Fc antibody (lower panel) as a positive control for all the recombinant proteins. Both 123C3 and Eric-1 specifically recognize the two FN repeats in NCAM ectodomain. (B) Lysates from SKOV3-mock or SKOV3-

NCAM cells were immunoblotted for phospho-FGFR (upper panels) and FGFR1 (lower panels), following the incubation with 123C3 or control mouse IgG1. SKOV3-mock cells were also stimulated with 10 ng/ml FGF-2 for 10 min. prior to lysis, as a control for FGFR activation. The blots were obtained from the same gel, the white line between the blots indicates the removal of intervening lanes. Ectopic NCAM expression promotes the activation of endogenous FGFR which, however, is abolished by the 123C monoclonal antibody. (C) HeLa cells were co-transfected with HA-tagged FGFR1 and either NCAM or an empty vector, as indicated. Cells were then incubated with 123C3, Eric-1 or control mouse IgG1, prior to cell lysis and immunoblotting with anti-phospho-FGFR (upper panel), anti-HA (middle panel), or anti-NCAM antibodies (lower panel). Ectopic NCAM expression results in the activation of HA-FGFR1, which is repressed by the 123C3 monoclonal antibody. The experiments were repeated three times with similar results.

Fig. S8. NCAM expression is retained in orthotopic EOC model. SKOV3 cells co-transfected with GFP and with an empty vector (mock; panels A and B), full-length NCAM (C and D) or NCAM-ΔFN2 (E and F) were injected orthotopically under the ovarian bursa of immunodeficient mice. Fourteen days after the injection, mice were sacrificed and adjacent sections of ovarian tissue were immunostained for NCAM (left panels) and GFP (right panels). Arrows indicate the primary tumor masses. The immunoreactive structures within the tumor mass in panel A most likely represent remnants of the NCAM-positive host ovarian stroma which has been disrupted by the growing tumor. Indeed, these structures show no GFP staining (panel B).

The pictures refer to the same samples shown in Fig. 5, and show representative images from one mouse per group. Four mice per group were used with similar results.

Fig. S9. NCAM-induced dissemination and vascular invasion in an orthotopic EOC model. (A) Representative image of GFP immunostaining on a SKOV3-NCAM tumor two weeks after orthotopic transplantation. The arrowhead indicate a disseminated lesion within extra-ovarian, fibro-adipose tissue. (B, C) Representative images of intravascular tumor cell emboli (arrowheads) in mice orthotopically transplanted with SKOV3-NCAM cells. Tissue sections were stained with hemataoxylin and eosin. (D, E) Intra-lymphatic tumor cell clusters in mice orthotopically transplanted with SKOV3-NCAM cells. Adjacent sections of the outer layer of the fallopian tube (i.e., extra-ovarian tissue) were stained for the lymphatic endothelial marker LYVE-1 (D) or for GFP (E). Arrowheads indicate a small tumor cell cluster within a LYVE-1-positive lymphatic vessel. Another tumor cell cluster, that does not appear to be intravascular, is shown in panel E.

Fig. S10. NCAM promotes peritoneal dissemination of EOC through its FGFR-binding domain. SKOV3 cells co-transfected with GFP and with an empty vector (mock; panels A), full-length NCAM (B) or NCAM-ΔFN2 (C) were injected into the peritoneum of nude mice. Tumor dissemination to the bowel was then assessed as described in Material and Methods. Light (left panels) and fluorescence images (right panels) of the same fields are shown. Scale bar, 1 mm.

Supplementary Figure S1

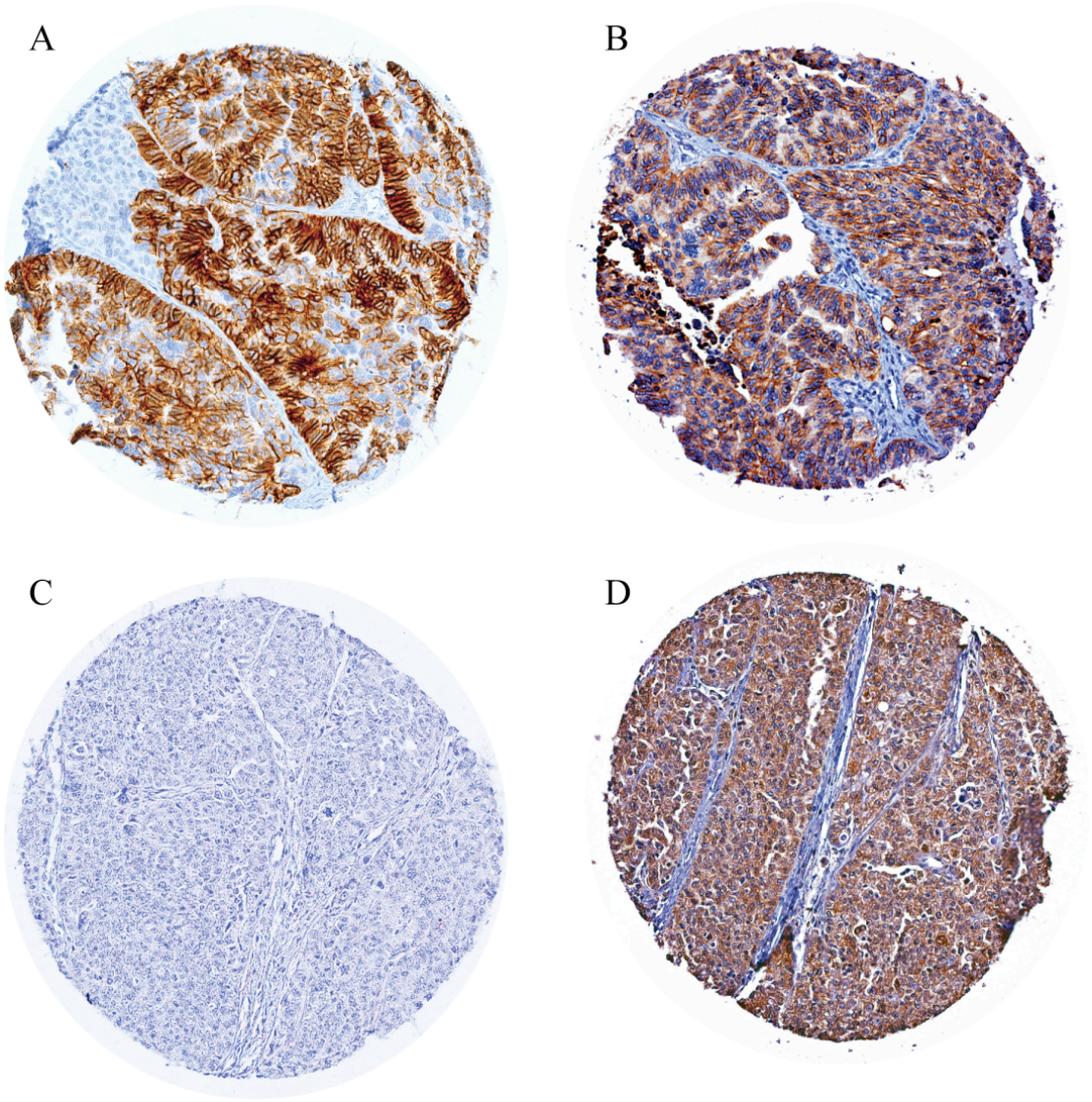

Supplementary Figure S2

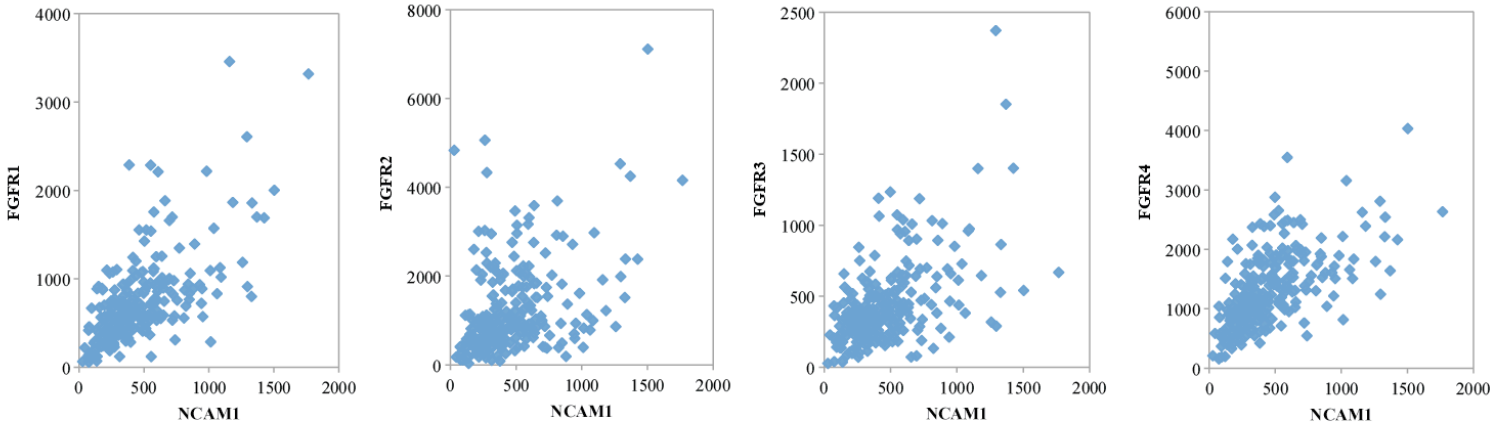

	NCAM/FGFR1	NCAM/FGFR2	NCAM/FGFR3	NCAM/FGFR4
Number of XY Pairs	255	255	255	255
Pearson r	0.6531	0.4086	0.5322	0.6137
95% confidence interval	0.5765 to 0.7183	0.3008 to 0.5060	0.4379 to 0.6148	0.5308 to 0.6849
P value (two-tailed)	< 0.0001	< 0.0001	< 0.0001	< 0.0001
Is the correlation significant? (alpha=0.05)	Yes	Yes	Yes	Yes
R square	0.4266	0.1669	0.2832	0.3766

Supplementary Figure S3

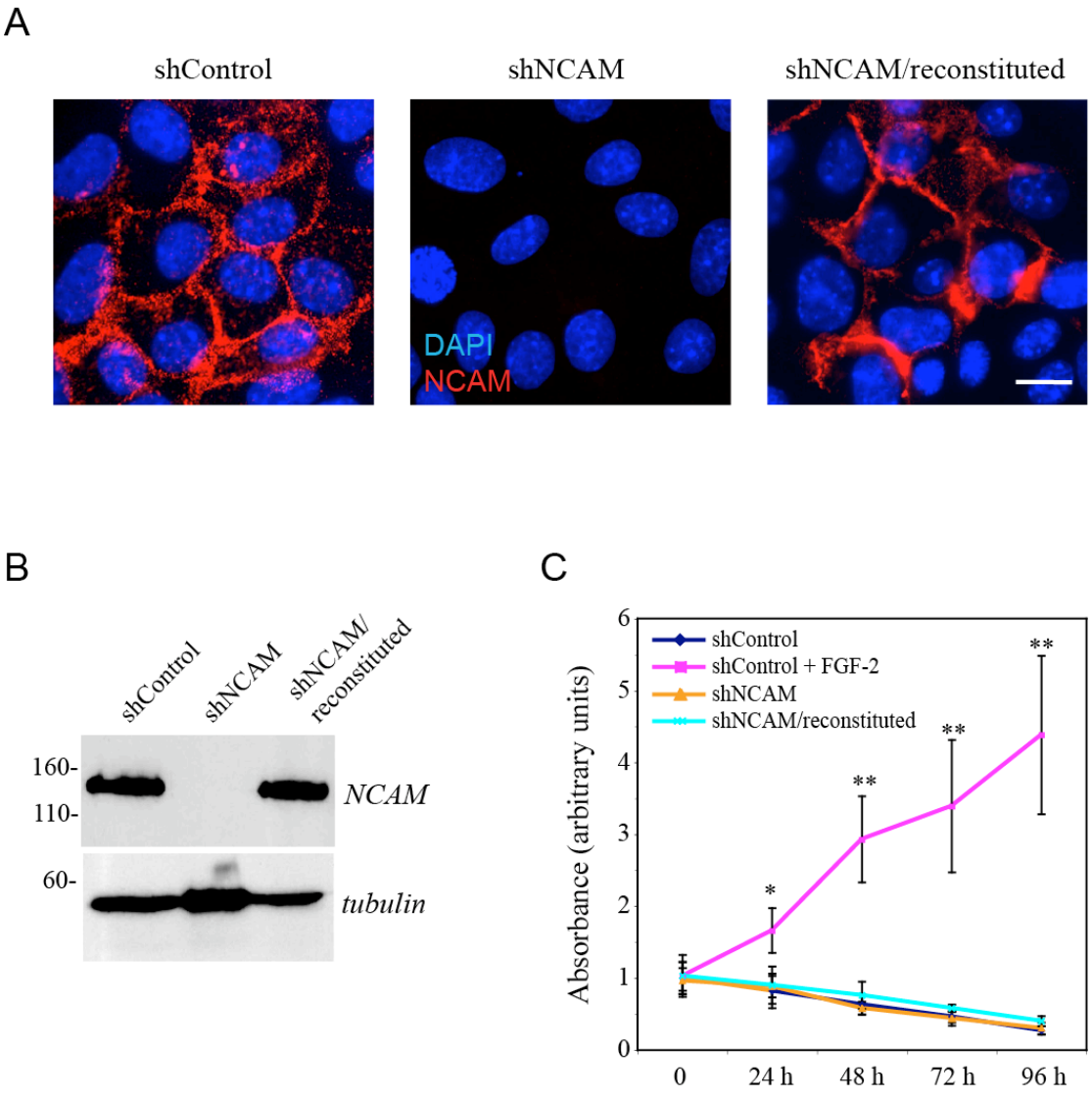

Supplementary Figure S4

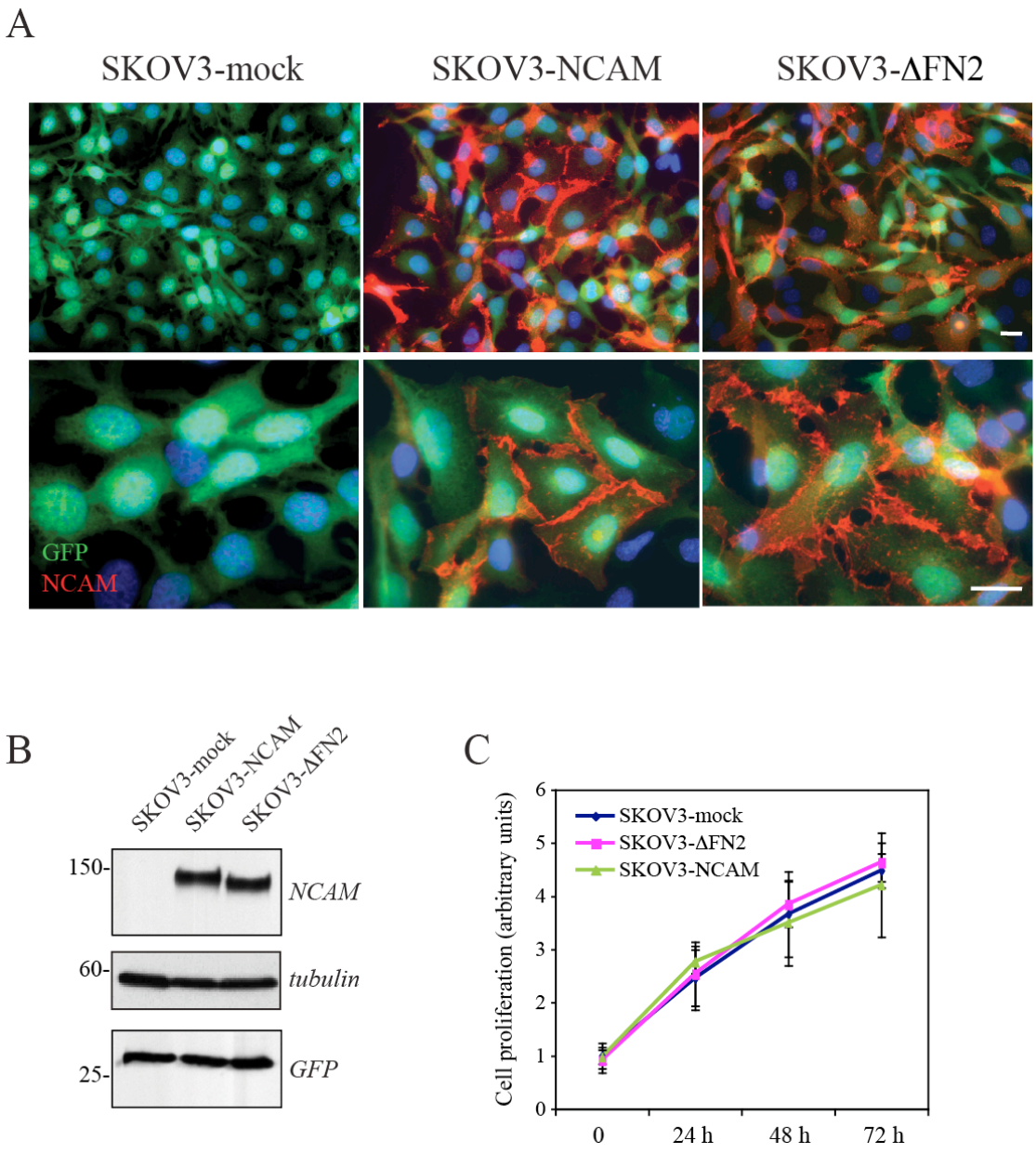

Supplementary Figure S5

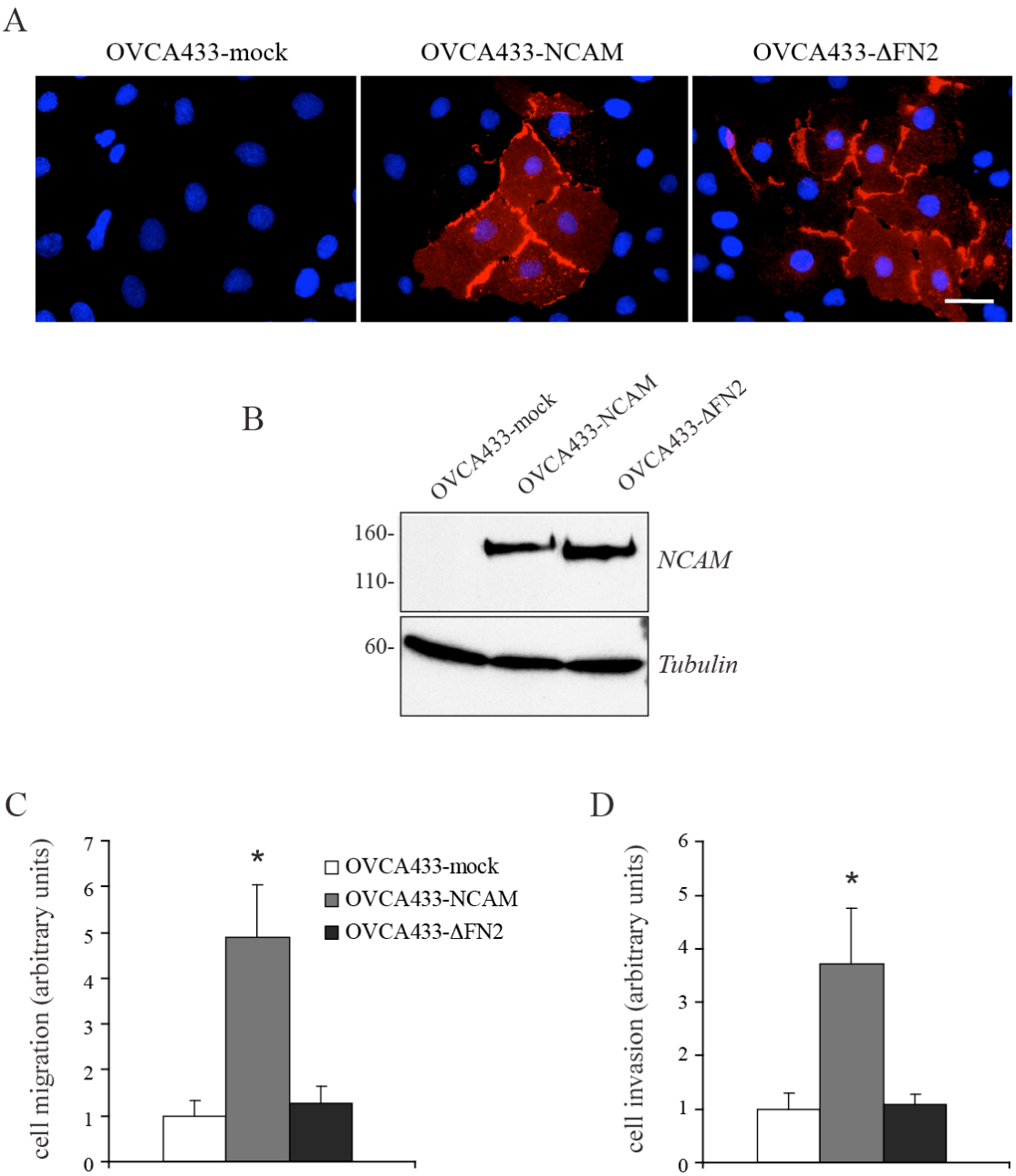

Supplementary Figure S6

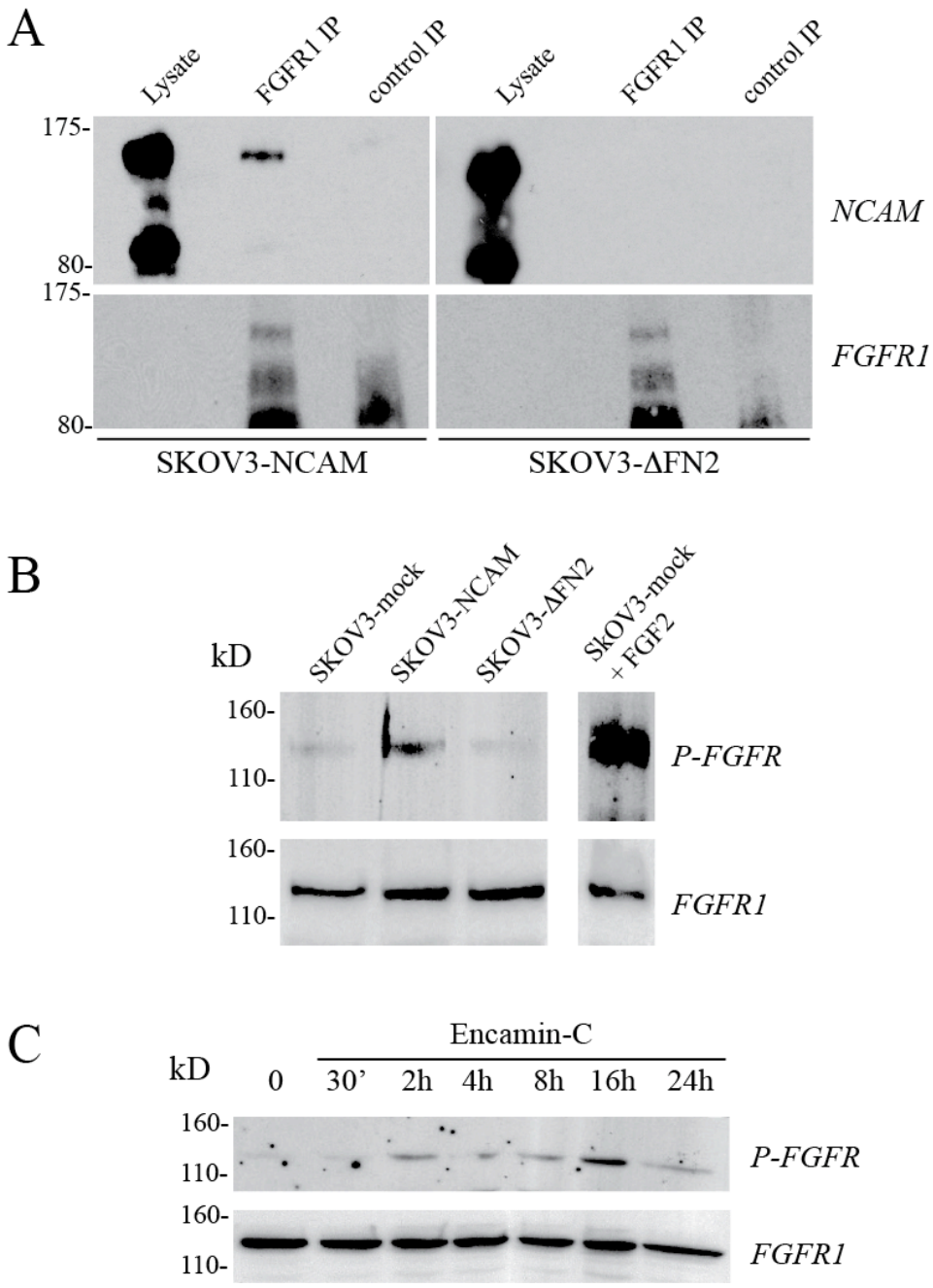

Supplementary Figure S7

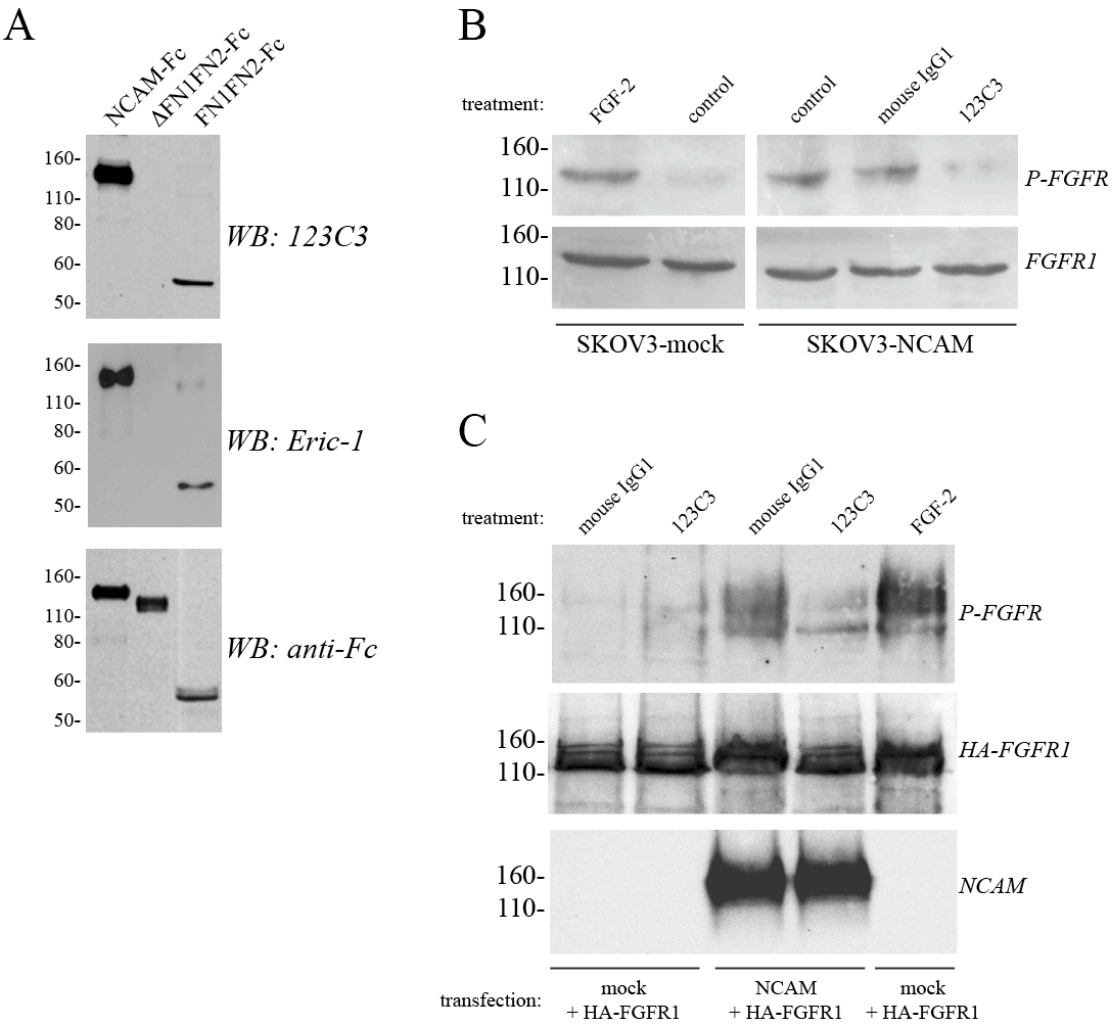

Supplementary Figure S8

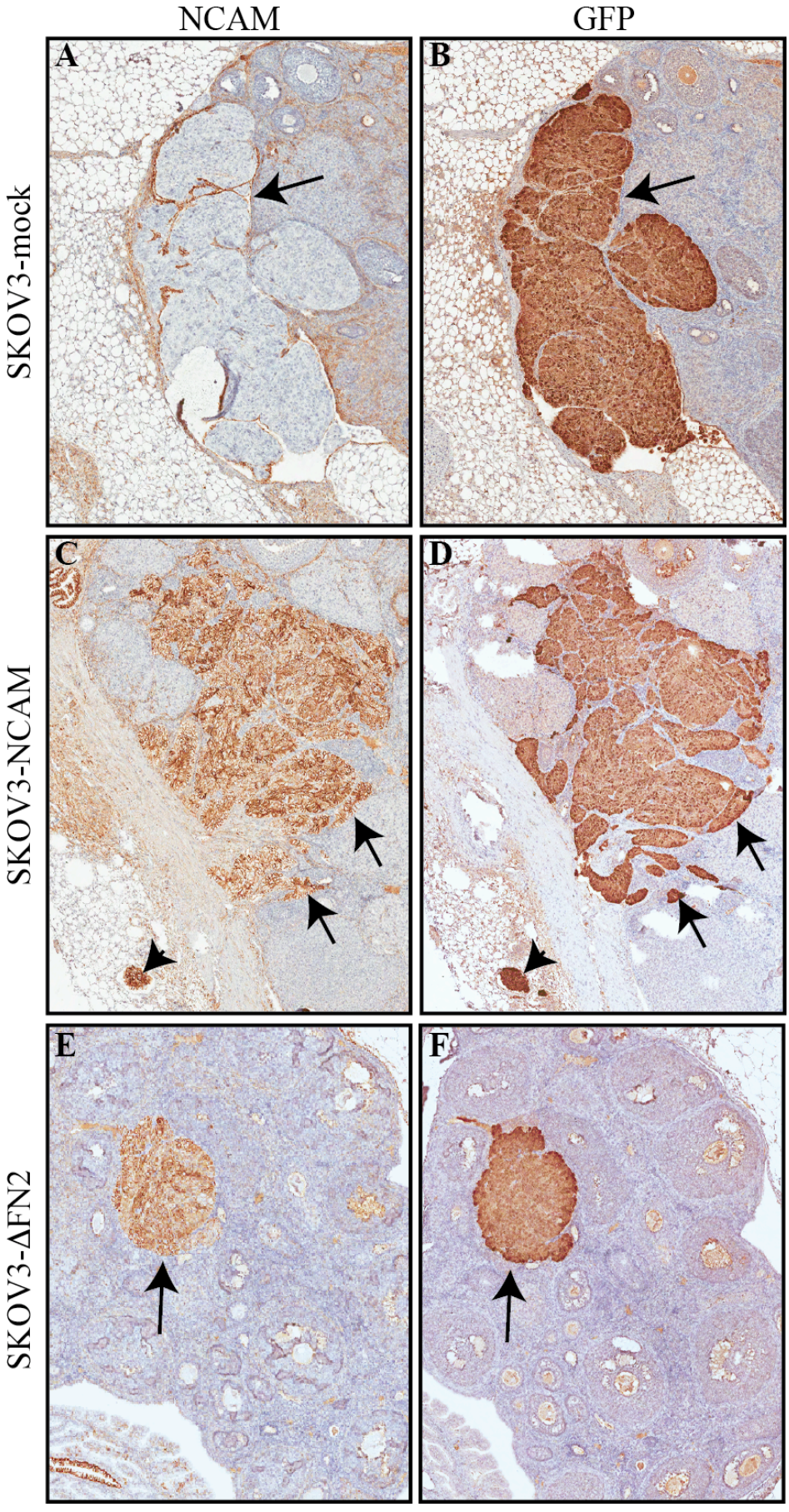

Supplementary Figure S9

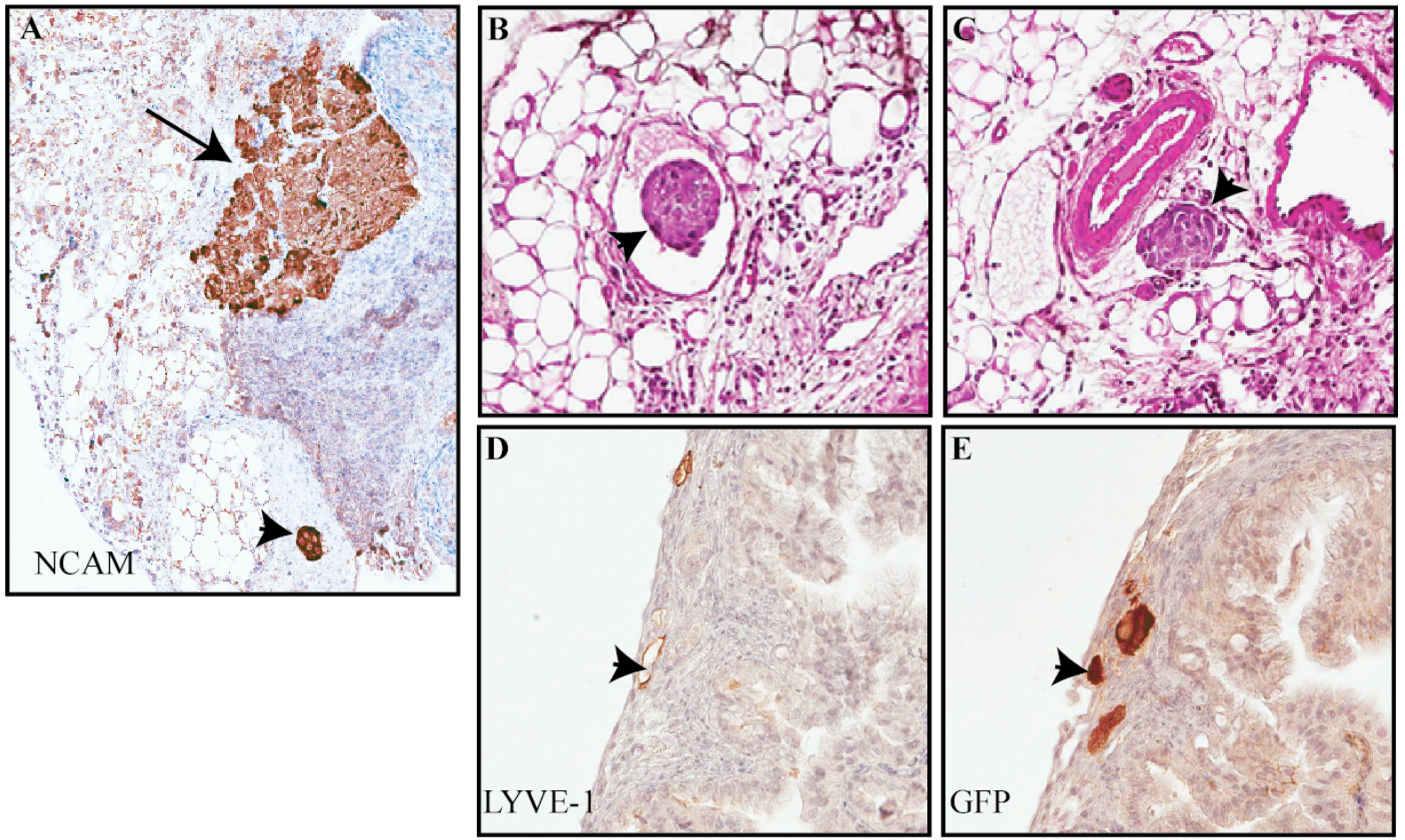

Supplementary Figure S10